

# Updated study of the $\eta_c$ and $\eta'_c$ decays into light vector mesons

Qian Wang<sup>1</sup>, Xiao-Hai Liu<sup>1</sup>, Qiang Zhao<sup>1,2</sup>

1) *Institute of High Energy Physics, Chinese Academy of Sciences, Beijing 100049, P.R. China*

2) *Theoretical Physics Center for Science Facilities, CAS, Beijing 100049, China*

(Dated: March 28, 2012)

We re-investigate the exclusive decays of  $\eta_c$  and  $\eta'_c$  to a pair of light vector mesons, i.e.  $\eta_c(\eta'_c) \rightarrow VV$ . The long-distance intermediate meson loop (IML) effects are evaluated as a non-perturbative mechanism in addition to the short-distance  $c\bar{c}$  annihilation contributions. We show that both processes can be reasonably well constrained with the help of the available experimental data. Since  $\eta_c$  and  $\eta'_c$  are the spin-0 partners of  $J/\psi$  and  $\psi'$ , respectively, our study is useful for gaining insights into the pQCD helicity selection rule violations in charmonium decays and the long-standing “ $\rho\pi$  puzzle”.

PACS numbers: 13.25.Gv, 11.30.Hv

## I. INTRODUCTION

Our knowledge about the properties of  $\eta_c$  and  $\eta'_c$  is still limited. Although  $\eta'_c$  as the first radial excitation state of the  $\eta_c$  has been predicted and studied for a long time, it is very recently that we gained more detailed information about its decay properties in experiment at CLEO [1] and BES-III [2]. The exclusive decays of  $\eta_c$  and  $\eta'_c$  to a pair of light vector mesons are of great interests among many other properties of these two states. One reason is that the  $VV$  decay channel turns out to be one of the most important decay channels for both  $\eta_c$  and  $\eta'_c$ . For instance, the branching ratios for  $\eta_c \rightarrow VV$  are typically at order of  $10^{-3}$  to  $10^{-2}$ . In contrast, these decay channels should be suppressed by the so-called helicity selection rule (HSR) [3–5]. Such an observation of the HSR violation indicates the importance of QCD higher twist contributions or presence of a non-pQCD mechanism that violates the HSR. The contradiction between the data and the HSR expectations based on the perturbative QCD (pQCD) has drawn much attention, and various attempts have been made to understand the underlying dynamics [6–13].

Another reason is that  $\eta_c(\eta'_c)$  exclusive decays can also be closely related to the long-standing so-called “ $\rho\pi$  puzzle” in  $J/\psi(\psi') \rightarrow VP$ . The decays of  $J/\psi$  and  $\psi'$  into light hadrons are supposed to be via the valence  $c\bar{c}$  annihilations into three gluons in pQCD to the leading order at a typical distance of  $1/m_c$ . Thus, the following relation similar to that between  $J/\psi$  and  $\psi'$  can be expected:

$$R_{\eta_c\eta'_c} \equiv \frac{BR(\eta'_c \rightarrow 2g)}{BR(\eta_c \rightarrow 2g)} = \frac{BR(\eta'_c \rightarrow \gamma\gamma)}{BR(\eta_c \rightarrow \gamma\gamma)}. \quad (1)$$

In the heavy quark limit, i.e.  $m_c$  is infinitely large, the mass difference between  $\eta_c$  and  $\eta'_c$  can be neglected. Hence, the branching ratio fraction becomes

$$R_{\eta_c\eta'_c} \simeq \left| \frac{\eta'_c(0)}{\eta_c(0)} \right|^2 \frac{\Gamma_{tot}^{\eta_c}}{\Gamma_{tot}^{\eta'_c}}, \quad (2)$$

similar to the “12% rule” between the  $J/\psi$  and  $\psi'$  decays. In the above equation  $\eta_c(0)$  and  $\eta'_c(0)$  are the values of the  $\eta_c$  and  $\eta'_c$  wavefunctions at their origins, respectively. On the other hand, in terms of the leading contributions from a potential quark model, deviations can be expected and one has

$$R_{\eta_c\eta'_c} = \left( \frac{M_{\eta_c}}{M_{\eta'_c}} \right)^2 \left| \frac{\eta'_c(0)}{\eta_c(0)} \right|^2 \frac{\Gamma_{tot}^{\eta_c}}{\Gamma_{tot}^{\eta'_c}}, \quad (3)$$

where the kinematic corrections cannot be neglected.

In the case of the  $J/\psi$  and  $\psi'$  decays, many theoretical efforts have been made in order to understand the origin of a significant deviation from the “12% rule” in  $J/\psi(\psi') \rightarrow \rho\pi$  and  $K^*\bar{K} + c.c.$  In recent works [14–16], we show that the interferences between the strong and EM decay amplitudes in both  $J/\psi(\psi') \rightarrow VP$  are essential for understanding the “ $\rho\pi$  puzzle”. Similar ideas had been proposed in the literature [17, 18]. A numerical study of the overall decay channels for  $J/\psi(\psi') \rightarrow VP$  indeed suggests such a phenomenon [15]. In Ref. [16], it is shown that the intermediate charmed meson loops can be considered as a long-distance effect to suppress the strong transition amplitudes due to their destructive interference with the short-distance strong transition amplitude in the  $\psi'$  decays.

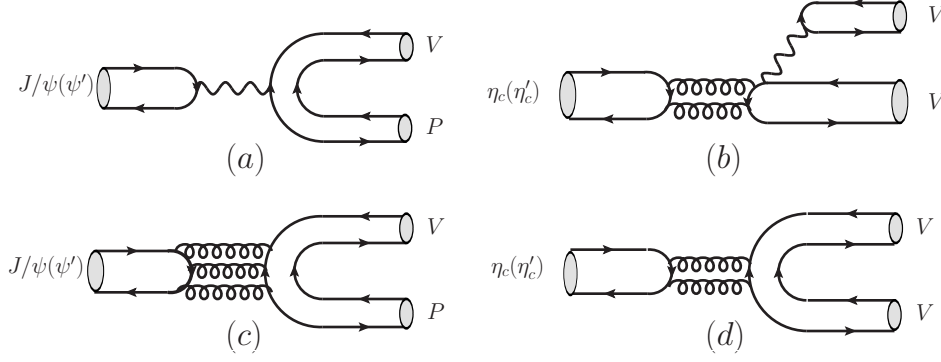


FIG. 1: Schematic diagrams for the EM and strong decays of  $J/\psi(\psi') \rightarrow VP$  and  $\eta_c(\eta'_c) \rightarrow VV$ .

As the spin-0 partner of  $J/\psi(\psi')$ , the decays of  $\eta_c(\eta'_c) \rightarrow VV$  provide an alternative way to examine the role played by the intermediate meson loop (IML) effects in the explanation of the “ $\rho\pi$  puzzle”. In Ref. [19], due to the lack of experimental data at that moment, the long-distance IML could not be well constrained, and it was assumed that the IML contributed about 10% of the amplitudes in  $\eta_c \rightarrow VV$  channel. With the recent availability of experimental data from BES-III [2], we can fit five channels of  $\eta_c \rightarrow VV$ , i.e.  $\omega\omega$ ,  $\phi\phi$ ,  $K^*\bar{K}^*$ ,  $\rho\rho$  and  $\omega\phi$ , to constrain both the short and long-distance contributions. The short-distance contribution in  $\eta'_c \rightarrow VV$  can thus be extracted by the ratio of the wave functions at the origin between  $\eta'_c$  and  $\eta_c$ . At the same time, the evolution of the IML to  $\eta'_c$  gives the long-distance contribution in  $\eta'_c \rightarrow VV$ . Note that the EM contributions via Fig. 1(b) is negligibly small in comparison with the strong ones via Fig. 1(d). It makes the decays of  $\eta_c(\eta'_c) \rightarrow VV$  an ideal place to single out the roles played by the short and long-distance strong transitions.

As follows, we will first provide the details of our formulations for the short and long-distance IML transitions in Sec. II. The numerical results and analysis are presented in Sec. III, and a brief summary is given in the last section.

## II. THE MODEL

This section provides the details of our theoretical approach for  $\eta_c(\eta'_c) \rightarrow VV$ . The first part is a parametrization of the short-distance contributions via hard gluon radiations in  $\eta_c(\eta'_c) \rightarrow VV$  when the  $c$  and  $\bar{c}$  annihilate at the wavefunction origin. The second part is the intermediated charmed meson loop transitions which account for the long-distance contributions. Namely, it describes non-negligible light quark pair creations before the  $c\bar{c}$  annihilation. These two mechanisms, in principle, have no double counting in the decays.

### A. The parametrization for $\eta_c(\eta'_c) \rightarrow VV$

An obvious advantage for the exclusive decays of  $\eta_c(\eta'_c) \rightarrow VV$  is that these transitions, similar to  $J/\psi(\psi') \rightarrow VP$ , have only one unique Lorentz structure for the  $VVP$  couplings. As stressed a number of times before, this will allow a parametrization of the effective coupling constant contributed by different mechanisms. In Ref. [9], a parametrization scheme is proposed for the short-distance transitions where the Okubo-Zweig-Iizuka singly disconnected (SOZI) and doubly disconnected (DOZI) processes can be parameterized by the gluon counting rule.

Following Ref. [9], the transition amplitudes for  $\eta_c \rightarrow VV$  can be expressed as

$$\begin{aligned}
 \langle \phi\phi | \hat{V}_{gg} | \eta_c \rangle &= gR^2(1+r) \\
 \langle \omega\omega | \hat{V}_{gg} | \eta_c \rangle &= g(1+2r) \\
 \langle \omega\phi | \hat{V}_{gg} | \eta_c \rangle &= grR\sqrt{2} \\
 \langle K^{*+}K^{*-} | \hat{V}_{gg} | \eta_c \rangle &= gR \\
 \langle \rho^+\rho^- | \hat{V}_{gg} | \eta_c \rangle &= g.
 \end{aligned} \tag{4}$$

where  $\hat{V}_{gg}$  is the  $\eta_c \rightarrow gg \rightarrow (q\bar{q})(q\bar{q})$  potential, and parameter  $g$  denotes the coupling strength of the SOZI transitions. Parameter  $r$  is the ratio of the DOZI transition over the SOZI transition. It should be pointed out that the additional gluon exchanges in DOZI are not necessarily perturbative. However, since they are higher twist contributions we

expect that their contributions would be small. This effect can be parameterized by  $r$ , of which a small value suggests a suppressed DOZI contribution [9]. We also introduce the SU(3) flavor breaking parameter  $R$ , of which its deviation from unity reflects the change of couplings due to the mass difference between  $u/d$  and  $s$ . The amplitudes for other charge combinations of  $K^* \bar{K}^*$  and  $\rho\rho$  are implicated.

A commonly used form factor is adopted in the calculation of the partial decay widths:

$$\mathcal{F}^2(\mathbf{p}) = p^{2l} \exp(-\mathbf{p}^2/8\beta^2), \quad (5)$$

where  $\mathbf{p}$  and  $l$  are the three momentum and relative angular momentum of the final-state mesons, respectively, in the  $\eta_c$  rest frame. We adopt  $\beta = 0.5$  GeV, which is the same as in Refs. [20–24]. Such a form factor will largely account for the size effects from the spatial wavefunctions of the initial and final state mesons.

## B. Intermediate charmed meson loops

### 1. Formulation

A well-developed effective Lagrangian approach is applied to estimate the long-distance IML transition amplitudes [16, 25–27]. The Feynman diagrams for  $\eta_c$  decays into  $\rho\rho$ ,  $K^* \bar{K}^*$ ,  $\omega\omega$ , and  $\phi\phi$  via the intermediate charmed meson loops are illustrated in Fig. 2. The relevant effective Lagrangians are based on heavy quark symmetry which describe the couplings between  $S$ -wave charmonium states and charmed mesons [28, 29] as the following,

$$\mathcal{L}_2 = ig_2 Tr[R_{c\bar{c}} \bar{H}_{2i} \gamma^\mu \overleftrightarrow{\partial}_\mu \bar{H}_{1i}] + H.c., \quad (6)$$

where the  $S$ -wave charmonium states are expressed as

$$R_{c\bar{c}} = \left( \frac{1+\not{p}}{2} \right) (\psi^\mu \gamma_\mu - \eta_c \gamma_5) \left( \frac{1-\not{p}}{2} \right), \quad (7)$$

and the charmed and anti-charmed meson triplet are

$$H_{1i} = \left( \frac{1+\not{p}}{2} \right) [\mathcal{D}_i^{*\mu} \gamma_\mu - \mathcal{D}_i \gamma_5], \quad (8)$$

$$H_{2i} = [\bar{\mathcal{D}}_i^{*\mu} \gamma_\mu - \bar{\mathcal{D}}_i \gamma_5] \left( \frac{1-\not{p}}{2} \right), \quad (9)$$

with  $\mathcal{D}$  and  $\mathcal{D}^*$  denote the pseudoscalar ( $(D^0, D^+, D_s^+)$ ) and vector charmed mesons ( $(D^{*0}, D^{*+}, D_s^{*+})$ ), respectively. The Lagrangian describing the interactions between light mesons and charmed mesons reads

$$\begin{aligned} \mathcal{L} = & -ig_{\rho\pi\pi} \left( \rho_\mu^+ \pi^0 \overleftrightarrow{\partial}^\mu \pi^- + \rho_\mu^- \pi^+ \overleftrightarrow{\partial}^\mu \pi^0 + \rho_\mu^0 \pi^- \overleftrightarrow{\partial}^\mu \pi^+ \right) \\ & - ig_{\mathcal{D}^* \mathcal{D} \mathcal{P}} (\mathcal{D}^i \partial^\mu \mathcal{P}_{ij} \mathcal{D}_\mu^{*j\dagger} - \mathcal{D}_\mu^{*i} \partial^\mu \mathcal{P}_{ij} \mathcal{D}^{j\dagger}) + \frac{1}{2} g_{\mathcal{D}^* \mathcal{D}^* \mathcal{P}} \epsilon_{\mu\nu\alpha\beta} \mathcal{D}_i^{*\mu} \partial^\nu \mathcal{P}^{ij} \overleftrightarrow{\partial}^\alpha \mathcal{D}_j^{*\beta\dagger} \\ & - ig_{\mathcal{D} \mathcal{D} \mathcal{V}} \mathcal{D}_i^\dagger \overleftrightarrow{\partial}_\mu \mathcal{D}^j (V^\mu)_j^i - 2f_{\mathcal{D}^* \mathcal{D} \mathcal{V}} \epsilon_{\mu\nu\alpha\beta} (\partial^\mu \mathcal{V}^\nu)_j^i (\mathcal{D}_i^\dagger \overleftrightarrow{\partial}^\alpha \mathcal{D}^{*j\beta} - \mathcal{D}_i^{*\beta\dagger} \overleftrightarrow{\partial}^\alpha \mathcal{D}^j) \\ & + ig_{\mathcal{D}^* \mathcal{D}^* \mathcal{V}} \mathcal{D}_i^{*\nu\dagger} \overleftrightarrow{\partial}_\mu \mathcal{D}_\nu^{*j} (\mathcal{V}^\mu)_j^i + 4if_{\mathcal{D}^* \mathcal{D}^* \mathcal{V}} \mathcal{D}_{i\mu}^{*\dagger} (\partial^\mu \mathcal{V}^\nu - \partial^\nu \mathcal{V}^\mu)_j^i \mathcal{D}_\nu^{*j}, \end{aligned} \quad (10)$$

with the convention  $\epsilon^{0123} = +1$ . In the above equation  $\mathcal{P}$  and  $\mathcal{V}_\mu$  denote  $3 \times 3$  matrices for the pseudoscalar octet and vector nonet, respectively [30], i.e.

$$\mathcal{P} = \begin{pmatrix} \frac{\pi^0}{\sqrt{2}} + \frac{\eta}{\sqrt{6}} & \pi^+ & K^+ \\ \pi^- & -\frac{\pi^0}{\sqrt{2}} + \frac{\eta}{\sqrt{6}} & K^0 \\ K^- & \bar{K}^0 & -\sqrt{\frac{2}{3}}\eta \end{pmatrix}, \quad \mathcal{V} = \begin{pmatrix} \frac{\rho^0}{\sqrt{2}} + \frac{\omega}{\sqrt{2}} & \rho^+ & K^{*+} \\ \rho^- & -\frac{\rho^0}{\sqrt{2}} + \frac{\omega}{\sqrt{2}} & K^{*0} \\ K^{*-} & \bar{K}^{*0} & \phi \end{pmatrix}. \quad (11)$$

The following kinematic conventions are adopted,  $\eta_c(p) \rightarrow \mathcal{D}^{(*)}(p_1) \bar{\mathcal{D}}^{(*)}(p_3) [\mathcal{D}^{(*)}(p_2)] \rightarrow V(k) V(q)$ , where  $\mathcal{D}^{(*)}$  in the square bracket denotes the exchanged charmed meson in the triangle diagrams. The explicit expressions of the

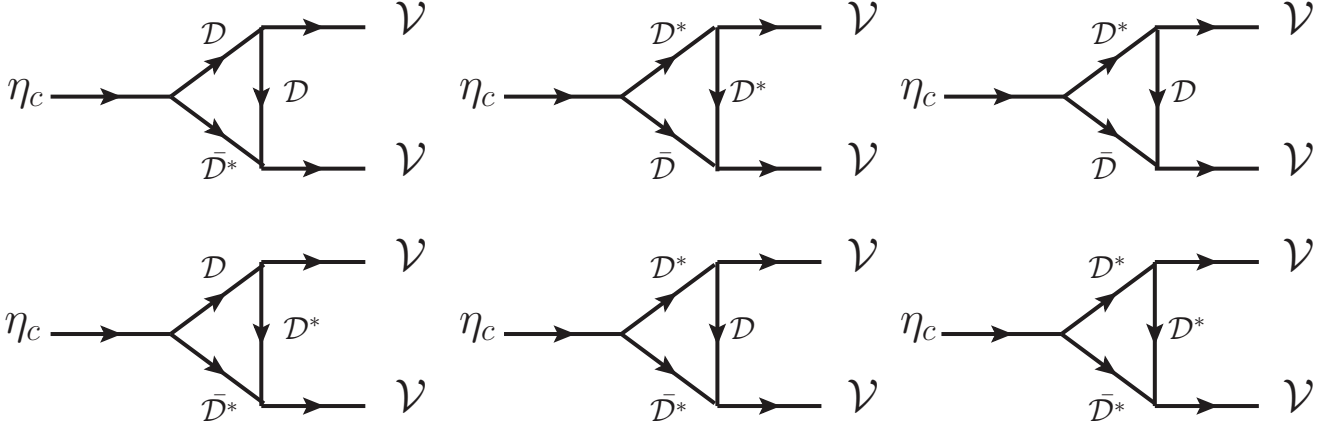


FIG. 2: Feynman diagrams for  $\eta_c \rightarrow VV$  via charmed meson loops. Here,  $\mathcal{D}$  and  $\mathcal{D}^*$  represent  $(D^+, D^0, D_s^+)$  and  $(D^{*+}, D^{*0}, D_s^{*+})$ , respectively, and  $\mathcal{V}$  denotes the light vector meson.

amplitudes are

$$\begin{aligned} \mathcal{M}_{\mathcal{D}\mathcal{D}^*[\mathcal{D}]} &= \int \frac{d^4 p_1}{(2\pi)^4} [-2g_{\eta_c \mathcal{D}\mathcal{D}^*} g_{\mathcal{D}\mathcal{D}\mathcal{V}} f_{\mathcal{D}\mathcal{D}^*} \epsilon_{\mu\nu\alpha\beta} (p_1 + p_2) \cdot \epsilon_k q^\mu \epsilon_q^\nu \\ &\quad \times (p_2 - p_3)^\alpha (p_1 - p_3)_\lambda (-g^{\lambda\beta} + \frac{p_3^\lambda p_3^\beta}{m_3^2})] \frac{1}{a_1 a_2 a_3} \mathcal{F}(p_i^2), \end{aligned} \quad (12)$$

$$\begin{aligned} \mathcal{M}_{\mathcal{D}\mathcal{D}^*[\mathcal{D}^*]} &= \int \frac{d^4 p_1}{(2\pi)^4} [-8g_{\eta_c \mathcal{D}\mathcal{D}^*} f_{\mathcal{D}\mathcal{D}^*} \epsilon_{\mu\nu\alpha\beta} k^\mu \epsilon_k^\nu (p_1 + p_2)^\alpha \\ &\quad \times (-g^{\beta\lambda} + \frac{p_2^\beta p_2^\lambda}{m_2^2}) (p_1 - p_3)_\delta (-g^{\delta\theta} + \frac{p_3^\delta p_3^\theta}{m_3^2}) (\epsilon_{q\lambda} q_\theta - q_\lambda \epsilon_{q\theta}) \\ &\quad + 2g_{\eta_c \mathcal{D}\mathcal{D}^*} f_{\mathcal{D}\mathcal{D}^*} g_{\mathcal{D}^* \mathcal{D}^* \mathcal{V}} \epsilon_{\mu\nu\alpha\beta} k^\mu \epsilon_k^\nu (p_1 + p_2)^\alpha (p_2 - p_3) \cdot \epsilon_q \\ &\quad \times (p_1 - p_3)_\delta (-g^{\beta\lambda} + \frac{p_2^\beta p_2^\lambda}{m_2^2}) (-g_\lambda^\delta + \frac{p_3^\lambda p_3^\delta}{m_3^2})] \frac{1}{a_1 a_2 a_3} \mathcal{F}(p_i^2), \end{aligned} \quad (13)$$

$$\begin{aligned} \mathcal{M}_{\mathcal{D}^* \mathcal{D}^*[\mathcal{D}]} &= \int \frac{d^4 p_1}{(2\pi)^4} [-4g_{\eta_c \mathcal{D}^* \mathcal{D}^*} f_{\mathcal{D}^* \mathcal{D}^*}^2 \epsilon_{\mu\nu\alpha\beta} \epsilon_{\rho\sigma\lambda\iota} \epsilon_{\eta\theta\xi\omega} p_1^\nu p_1^\mu (p_1 + p_2)^\lambda \\ &\quad \times k^\rho \epsilon_k^\sigma q^\eta \epsilon_q^\theta (p_2 - p_3)^\xi (-g^{\beta\iota} + \frac{p_1^\beta p_1^\iota}{m_1^2}) (-g^{\alpha\omega} + \frac{p_3^\alpha p_3^\omega}{m_3^2})] \frac{1}{a_1 a_2 a_3} \mathcal{F}(p_i^2), \end{aligned} \quad (14)$$

$$\mathcal{M}_{\mathcal{D}^* \mathcal{D}^*[\mathcal{D}^*]} = \int \frac{d^4 p_1}{(2\pi)^4} [\mathcal{A}_1 + \mathcal{A}_2 + \mathcal{A}_3 + \mathcal{A}_4] \frac{1}{a_1 a_2 a_3} \mathcal{F}(p_i^2),$$

where

$$\begin{aligned} \mathcal{A}_1 &\equiv g_{\eta_c \mathcal{D}^* \mathcal{D}^*} g_{\mathcal{D}^* \mathcal{D}^* \mathcal{V}}^2 \epsilon_{\mu\nu\alpha\beta} p_1^\mu (p_1 + p_2) \cdot \epsilon_k (p_2 - p_3) \cdot \epsilon_q \\ &\quad \times (-g^{\beta\lambda} + \frac{p_1^\beta p_1^\lambda}{m_1^2}) (-g_{\lambda\delta} + \frac{p_2^\lambda p_2^\delta}{m_2^2}) (-g^{\delta\alpha} + \frac{p_3^\delta p_3^\alpha}{m_3^2}), \\ \mathcal{A}_2 &\equiv -4g_{\eta_c \mathcal{D}^* \mathcal{D}^*} g_{\mathcal{D}^* \mathcal{D}^* \mathcal{V}} f_{\mathcal{D}^* \mathcal{D}^*} \epsilon_{\mu\nu\alpha\beta} p_1^\nu p_1^\mu (p_1 + p_2) \cdot \epsilon_k \\ &\quad \times (-g^{\beta\lambda} + \frac{p_1^\beta p_1^\lambda}{m_1^2}) (-g_{\lambda\rho} + \frac{p_2^\lambda p_2^\rho}{m_2^2}) (-g_\delta^\alpha + \frac{p_3^\delta p_3^\alpha}{m_3^2}) (\epsilon_q^\rho q^\delta - q^\rho \epsilon_q^\delta), \end{aligned} \quad (15)$$

$$\begin{aligned}
\mathcal{A}_3 &\equiv -4g_{\eta_c \mathcal{D}^* \mathcal{D}^*} g_{\mathcal{D}^* \mathcal{D}^* \mathcal{V}} f_{\mathcal{D}^* \mathcal{D}^* \mathcal{V}} \epsilon_{\mu\nu\alpha\beta} p_1^\nu p_1^\mu (-p_3 + p_2) \cdot \epsilon_q \\
&\times (-g_\lambda^\beta + \frac{p_1^\beta p_{1\lambda}}{m_1^2}) (-g_{\sigma\rho} + \frac{p_{2\sigma} p_{2\rho}}{m_2^2}) (-g^{\rho\alpha} + \frac{p_3^\rho p_3^\alpha}{m_3^2}) (k^\sigma \epsilon_k^\lambda - \epsilon_k^\sigma k^\lambda), \\
\mathcal{A}_4 &\equiv 16g_{\eta_c \mathcal{D}^* \mathcal{D}^*} f_{\mathcal{D}^* \mathcal{D}^* \mathcal{V}}^2 \epsilon_{\mu\nu\alpha\beta} p_1^\nu p_1^\mu (-g_\lambda^\beta + \frac{p_1^\beta p_{1\lambda}}{m_1^2}) (-g_\rho^\alpha + \frac{p_2^\alpha p_{2\rho}}{m_2^2}) \\
&\times (-g_{\theta\delta} + \frac{p_{3\theta} p_{3\delta}}{m_3^2}) (q^\rho \epsilon_k^\lambda k^\theta \epsilon_q^\delta + \epsilon_q^\rho k^\lambda q^\theta \epsilon_k^\delta - \epsilon_q^\rho \epsilon_k^\lambda q^\theta k^\delta - q^\rho k^\lambda \epsilon_k^\theta \epsilon_q^\delta),
\end{aligned}$$

with  $a_1 \equiv p_1^2 - m_1^2$ ,  $a_2 \equiv p_2^2 - m_2^2$ , and  $a_3 \equiv p_3^2 - m_3^2$ . The amplitudes  $\mathcal{M}_{\mathcal{D}^* \bar{\mathcal{D}}[\mathcal{D}]}$  and  $M_{\mathcal{D}^* \bar{\mathcal{D}}[\mathcal{D}^*]}$  have the same expressions as  $\mathcal{M}_{\mathcal{D} \bar{\mathcal{D}}[\mathcal{D}]}$  and  $M_{\mathcal{D} \bar{\mathcal{D}}[\mathcal{D}^*]}$ , respectively, and are omitted for brevity. The full expressions of the transition amplitudes for each  $VV$  mode can be found in the Appendix.

Since the couplings in the effective Lagrangians are local ones, ultra-violet divergence in the loop integrals is inevitable. We introduce a tri-monopole form factor  $\mathcal{F}(p_i^2)$  phenomenologically to take into account the non-local effects and cut off the divergence in the loop integrals, i.e.

$$\mathcal{F}(p_i^2) = \prod_i \left( \frac{\Lambda_i^2 - m_i^2}{\Lambda_i^2 - p_i^2} \right), \quad (16)$$

where  $m_i$  and  $p_i$  are the mass and four momentum of the corresponding exchanged particle, and the cut-off energy is chosen as  $\Lambda_i = m_i + \alpha \Lambda_{QCD}$  with  $\Lambda_{QCD} = 0.22$  GeV [26, 27, 30]. The value of parameter  $\alpha$  will generally be determined by experimental data.

## 2. Vertex couplings in the IML integrals

Before proceeding to the numerical results, we first determine some of the parameters included in this approach. In the chiral and heavy quark limit, the following relations can be obtained [29, 30],

$$g_{\mathcal{D} \mathcal{D} \mathcal{V}} = g_{\mathcal{D}^* \mathcal{D}^* \mathcal{V}} = \frac{\beta g_V}{\sqrt{2}}, \quad f_{\mathcal{D}^* \mathcal{D}^* \mathcal{V}} = \frac{f_{\mathcal{D}^* \mathcal{D}^* \mathcal{V}}}{m_{\mathcal{D}^*}} = \frac{\lambda g_V}{\sqrt{2}}, \quad g_V = \frac{m_\rho}{f_\pi}, \quad (17)$$

$$g_{\eta_c \mathcal{D} \mathcal{D}^*} = g_{\eta_c \mathcal{D}^* \mathcal{D}^*} \sqrt{\frac{m_{\mathcal{D}}}{m_{\mathcal{D}^*}}} m_{\eta_c} = 2g_2 \sqrt{m_{\eta_c} m_{\mathcal{D}} m_{\mathcal{D}^*}}, \quad (18)$$

where  $\beta$  and  $\lambda$  are commonly taken as  $\beta = 0.9$ ,  $\lambda = 0.56$  GeV<sup>-1</sup>, while  $f_\pi$  is the pion decay constant.

In principle, the coupling  $g_2$  should be computed by nonperturbative methods. If we simply estimate it with the vector meson dominance (VMD) argument, it gives  $g_2 = \sqrt{m_{\psi}}/(2m_{\mathcal{D}} f_\psi)$ , where  $m_\psi$  and  $f_\psi = 405$  MeV being the mass and decay constant of  $J/\psi$  [28]. This relation gives  $g_{\eta_c \mathcal{D} \mathcal{D}^*} = 7.68$ , which is a commonly adopted value in the literature. For simplicity, we assume that  $g_{\eta_c \mathcal{D} \mathcal{D}^*}/g_{\eta_c' \mathcal{D} \mathcal{D}^*} = 1$  and it is also applied to the  $\eta_c(\eta_c')$  coupling to  $\mathcal{D}^* \mathcal{D}^*$ .

It should be mentioned again that the decays  $\eta_c(\eta_c') \rightarrow VV$  are strong-interaction-dominant processes with negligible EM contributions. They are different from the decays  $J/\psi(\psi') \rightarrow VP$  where the EM interaction may still play an important role, especially in  $\psi' \rightarrow VP$  [14, 15]. As shown in Fig. 1, a naive power counting indicates that

$$\begin{aligned}
\frac{\mathcal{M}_{em}}{\mathcal{M}_{strong}} &\sim \frac{\alpha_e}{\alpha_s^2} \quad \text{for } J/\psi(\psi') \rightarrow VP, \\
\frac{\mathcal{M}_{em}}{\mathcal{M}_{strong}} &\sim \alpha_e \quad \text{for } \eta_c(\eta_c') \rightarrow VV,
\end{aligned} \quad (19)$$

where “ $\mathcal{M}_{em}$ ” and “ $\mathcal{M}_{strong}$ ” denote the leading EM and strong transition amplitudes, respectively. It implies that the EM contribution in  $\eta_c(\eta_c') \rightarrow VV$  will be less important than that in  $J/\psi(\psi') \rightarrow VP$ . As a result, the total (strong) amplitude of  $\eta_c(\eta_c') \rightarrow VV$  can be expressed as

$$\mathcal{M}_{tot}(\eta_c(\eta_c')) = \mathcal{M}_{short} + e^{i\theta(\theta')} \mathcal{M}_{long}, \quad (20)$$

where  $\mathcal{M}_{short}$  and  $\mathcal{M}_{long}$  are the short and long-distance amplitude, respectively, and  $\theta$  ( $\theta'$ ) is the relative phase angle for the  $\eta_c(\eta_c')$  decays. In principle,  $\theta(\theta')$  should be 0° or 180° which provide an arbitrary sign between those two real amplitudes. Deviations from 0° or 180° imply that intermediate light meson loops might have contributions. Note that the  $VVP$  coupling has only one unique Lorentz structure. Any possible contributions would be absorbed into

TABLE I: The parameters in our model have been fitted in  $\eta_c \rightarrow VV$  processes. The reduced chi-square is also given in this table.

parameter	value
$g_{\eta_c}$	$(3.913 \pm 1.03) \times 10^{-2}$
$R$	$0.854 \pm 0.158$
$r$	$-0.154 \pm 0.117$
$\theta$	$174.29 \pm 91.798$
$\alpha$	$0.30 \pm 0.151$
$\chi^2$	3.67

the effective coupling constant. By freeing  $\theta(\theta')$ , the imaginary amplitudes, if necessary, would indirectly reflect the intermediate light meson loops. We mention in advance that the data fitting for  $\eta_c \rightarrow VV$  favors that  $\theta \simeq 180^\circ$ , which indicates that the light meson loops are rather small. This contribution can be better studies given the availability of more precise measurement of the branching ratios.

### III. NUMERICAL RESULTS AND ANALYSIS

There are five explicit parameters to be determined in  $\eta_c \rightarrow VV$ , among which three are from the short-distance transitions, i.e. the SOZI strength  $g$ , the SU(3) breaking parameter  $R$ , and the DOZI parameter  $r$ , while two are from the long-distance IML transitions, i.e. the cut-off parameter  $\alpha$  and the relative angle  $\theta$  between the short-distance and the long-distance amplitudes. In contrast, other parameters in the previous section have been determined independently and are treated as inputs.

It appears to be possible to constrain those parameters for  $\eta_c \rightarrow VV$  given the availability of the experimental data for five decay channels. For the  $\eta_c \rightarrow \omega\omega$  and  $\omega\phi$  channel, we use the half values of the up limits in our fitting scheme. As follows, we first do a numerical fit of the data and analyze the implicated constraints on the underlying dynamics.

In Table I the fitted parameters are listed. The following points can be learned from the fitted results:

- The SOZI strength,  $g_{\eta_c} = (3.913 \pm 1.03) \times 10^{-2}$ , is larger than  $g_{J/\psi} = 1.75 \times 10^{-2}$  determined in  $J/\psi \rightarrow VP$  [16]. Since  $c\bar{c}$  annihilate through three gluons in  $J/\psi$  decays and through two gluons in  $\eta_c$  decays, this SOZI parameter satisfies approximately the relation established by the inclusive strong decay widths for  $J/\psi \rightarrow 3g$  and  $\eta_c \rightarrow 2g$ .
- The SU(3) flavor symmetry breaking parameter  $R$  is generally estimated by  $f_\pi/f_K \sim 0.838$ , with  $f_\pi$  and  $f_K$  the decay constants of pion and kaon. As shown in Table I, the fitted value  $R = 0.854 \pm 0.158$  is consistent with the decay constant ratio.
- The DOZI parameter  $r \sim -0.154$  is consistent with that extracted in Refs. [9, 16]. It suggests that the short-distance SOZI is dominant in  $\eta_c \rightarrow VV$ . In contrast with  $J/\psi \rightarrow VP$ , the ambiguity due to the possible glueball component inside the  $\eta$  and  $\eta'$  can be avoided.
- It shows that there are large uncertainties with the relative phase between the short and long-distance amplitudes. This suggests that contributions from the long-distance IML transitions are relatively small in  $\eta_c \rightarrow VV$ . In comparison with  $J/\psi \rightarrow VP$  the IML contributions do not have much freedom since the vertex couplings in these two processes are correlated in the limit of heavy quark symmetry. It is thus natural to expect that the value of the form factor parameter  $\alpha$  is in a similar range as that determined in  $J/\psi \rightarrow VP$ . In this work, by relaxing slightly the boundary values for  $\alpha$ , i.e. with  $\alpha = 0.30 \pm 0.151$ , we find that the reduced  $\chi^2$  can be improved significantly.

In Table II the fitted branching ratios are listed and compared with the experimental data [31]. The central value of the total decay width  $\Gamma_{\eta_c} = 28.6 \pm 2.2$  MeV is adopted. The branching ratios from the exclusive short and long-distance transitions are also listed. It shows that the short-distance transitions are dominant in  $\eta_c \rightarrow VV$  as expected, while the IML contributions are rather small since the  $\eta_c$  mass is far away from the open charm threshold.

With the above determined parameters for the short and long-distance transition amplitudes in  $\eta_c \rightarrow VV$ , we now extend the calculation to  $\eta'_c \rightarrow VV$ .

As discussed earlier, the short-distance decay amplitudes for  $\eta_c$  and  $\eta'_c$  are proportional to their wavefunctions at the origins. They are spin-0 partner of  $J/\psi$  and  $\psi'$ , respectively. Therefore, the ratio of the wavefunctions at their origins can be related to that for  $J/\psi$  and  $\psi'$ , i.e.  $|\eta'_c(0)|/|\eta_c(0)| \simeq |\psi_{2S}(0)|/|\psi_{1S}(0)|$ . It has been broadly



discussed in the literature [32–34] that  $|\psi_{2S}(0)|/|\psi_{1S}(0)|$  can be extracted from either the mass splitting between the  $^1S_0$  and  $^3S_1$  state or the lepton pair decay widths of  $\psi_{2S}$  and  $\psi_{1S}$ . For instance, the estimate of Ref. [32] gives  $|\psi_{2S}(0)|^2/|\psi_{1S}(0)|^2 = 0.62 \pm 0.16$ . By adopting  $|\eta'_c(0)|/|\eta_c(0)| \simeq |\psi_{2S}(0)|/|\psi_{1S}(0)|$ , we can determine the magnitude of the short-distance amplitudes for  $\eta'_c \rightarrow VV$  via the  $\eta_c$  decays.

For the long-distance transition amplitude, the form factor parameter  $\alpha_{\eta'_c}$  cannot be well constrained. However, one can determine its upper limit based on the properties of the meson loop integrals. In comparison with the IML in  $\eta_c \rightarrow VV$ , the IML integrals in  $\eta'_c \rightarrow VV$  involves the change of the first vertex couplings, i.e.  $\eta'_c \mathcal{D}\mathcal{D}^*$  and  $\eta'_c \mathcal{D}^*\mathcal{D}^*$ , and the initial mass change from  $\eta_c$  to  $\eta'_c$ . Apart from the vertex couplings, the initial mass change will lead to enhanced IML contributions if the same form factor parameter  $\alpha_{\eta'_c} = \alpha_{\eta_c}$  is adopted. Due to this feature, we will also investigate the sensitivities of the predictions within  $\alpha_{\eta'_c} = \alpha_{\eta_c} = 0.30 \pm 0.151$ . This should be a reasonable range for the estimate of the upper limit of the long-distance IML contributions with an uncertainty.

The last parameter, the relative phase angle  $\theta'$  between the short and long-distance amplitudes, is a free one in this formulation. Taking into account the uncertainties with the values of  $|\eta'_c(0)|$  and  $\alpha_{\eta'_c}$ , we study two situations of  $\theta'$ -dependence of the branching ratios for  $\eta'_c \rightarrow VV$  as follows.

First, in Fig. 3 we fix  $\alpha_{\eta'_c} = \alpha_{\eta_c} = 0.30$  and explore the  $\theta'$ -dependence of the branching ratios. The shadowed bands are the range given by the uncertainties due to the value of the wavefunction at the origin, i.e.  $|\eta'_c(0)|/|\eta_c(0)| \simeq |\psi_{2S}(0)|/|\psi_{1S}(0)| = 0.62 \pm 0.16$ . The solid lines are the experimental upper limits from the BES-III experiment [2]. It shows that for those measured channels, i.e.  $\eta'_c \rightarrow K^{*0}\bar{K}^{*0}$ ,  $\rho^0\rho^0$ , and  $\phi\phi$ , the predicted branching ratios are consistent with the experimental limits. In fact, the contributions from the long-distance IML transitions are still relatively smaller than those from the short-distance ones. Therefore, the interferences at different relative phase angles cause only about 20% deviations.

Secondly, in Fig. 4, we fix the central value  $|\eta'_c(0)|/|\eta_c(0)| = 0.62$  and explore the  $\theta'$ -dependence of the branching ratios within the range of  $\alpha_{\eta'_c} = 0.30 \pm 0.151$ . By comparing the values at  $\theta' = 0^\circ$  in Figs. 3 and 4, we can see that the uncertainties with  $|\eta'_c(0)|$  and  $\alpha_{\eta'_c}$  cause similar magnitude of uncertainties with the predicted branching ratios. Since both the short and long-distance amplitudes are calculated as real quantities, the nodes structures at  $\theta' = 90^\circ$  and  $270^\circ$  in Fig. 4 locate the phase angles that the IML transitions only contribute to the imaginary part. Since the magnitude is small, its changes to the predicted branching ratios are not significant. In contrast, at  $\theta' = 0^\circ$  or  $180^\circ$ , the IML transitions contribute to the real part with different signs. Its interferences are amplified by the short-distance amplitude, thus lead to much larger effects to the predictions as shown by the shadowed areas.

The following points can be further learned in order:

- In  $\eta'_c \rightarrow VV$  the relative strength of the IML amplitudes to the short-distance ones is not as large as that in  $\psi' \rightarrow VP$ . This should be understandable due to the different open charm thresholds in  $\psi' \rightarrow VP$  and  $\eta'_c \rightarrow VV$ . For the latter process, the first open charm threshold is  $D^*\bar{D} + c.c.$ , while for  $\psi' \rightarrow VP$  it is  $D\bar{D}$ . As a consequence, the dominance of the short-distance contributions can make the relations by Eqs. (1) and (3) to be satisfied. It is unlikely to have a drastic variation of the ratios as observed in  $J/\psi$  and  $\psi' \rightarrow VP$  [16].
- Since the long-distance IML transitions do not contribute to the  $\omega\phi$  decay mode at leading order, it is interesting to recognize that a precise measurement of  $BR(\eta_c(\eta'_c) \rightarrow \omega\phi)$  would provide a strong constraint on the short-distance process. In particular, it will constrain the DOZI transition parameter  $r$  in  $\eta'_c \rightarrow VV$ . By adopting the value  $r = -0.154 \pm 0.117$  determined in  $\eta_c \rightarrow VV$ , we predict  $BR(\eta'_c \rightarrow \omega\phi) = (1.82 \pm 0.47) \times 10^{-4}$ , which can be tested by future BES-III data.

Combining these two decays together, i.e.  $\eta_c(\eta'_c) \rightarrow VV$  and  $J/\psi(\psi') \rightarrow VP$  [16], we find that the IML transitions do not contribute strongly in  $\eta'_c \rightarrow VV$  compared with those in  $\psi' \rightarrow VP$  because of the difference of open charm thresholds. In contrast, the IML contributions in both  $\eta_c \rightarrow VV$  and  $J/\psi \rightarrow VP$  are rather small. As discussed before that the EM contribution can be neglected in  $\eta_c(\eta'_c) \rightarrow VV$ , the relatively small contribution from the long-distance IML implies that Eq.(1) would be well respected. We stress that our investigation suggests that the same IML mechanism would have rather different manifestations in different processes. Therefore, a systematic study of those correlated processes is essential for a better understanding of the HSR violation and disentangling the long-standing “ $\rho\pi$  puzzle”.

#### IV. SUMMARY

In this work, we have studied the decay properties of  $\eta_c$  and  $\eta'_c \rightarrow VV$  as an alternative process for the test of intermediate meson loop transitions. The availability of experimental data for  $\eta_c \rightarrow VV$  allows the determination of our model parameters which then can be used as inputs in  $\eta'_c \rightarrow VV$ . Nevertheless, we show that the correlation between  $\eta_c(\eta'_c) \rightarrow VV$  and  $J/\psi(\psi') \rightarrow VP$  is essentially important for isolating the short and long-distance transition

TABLE II: Branching ratios of  $\eta_c \rightarrow VV$  in comparison with the experimental data [31]. The exclusive branching ratios from the short and long-distance transitions are also included. The total width  $\Gamma_{\eta_c} = 28.6$  MeV is adopted.

$BR(\eta_c \rightarrow VV)$	short-distance	long-distance	tot.	exp.
$\omega\omega$	$1.92 \times 10^{-3}$	$3.2 \times 10^{-6}$	$1.76 \times 10^{-3}$	$< 3.1 \times 10^{-3}$
$\phi\phi$	$2.1 \times 10^{-3}$	$2.33 \times 10^{-6}$	$1.96 \times 10^{-3}$	$(2.7 \pm 0.9) \times 10^{-3}$
$K^*\bar{K}^*$	$1.34 \times 10^{-2}$	$1.09 \times 10^{-5}$	$1.27 \times 10^{-2}$	$(9.2 \pm 3.4) \times 10^{-3}$
$\rho\rho$	$1.19 \times 10^{-2}$	$9.53 \times 10^{-6}$	$1.13 \times 10^{-2}$	$(2.0 \pm 0.7) \times 10^{-2}$
$\omega\phi$	$3.25 \times 10^{-4}$	0	$3.25 \times 10^{-4}$	$< 1.7 \times 10^{-3}$

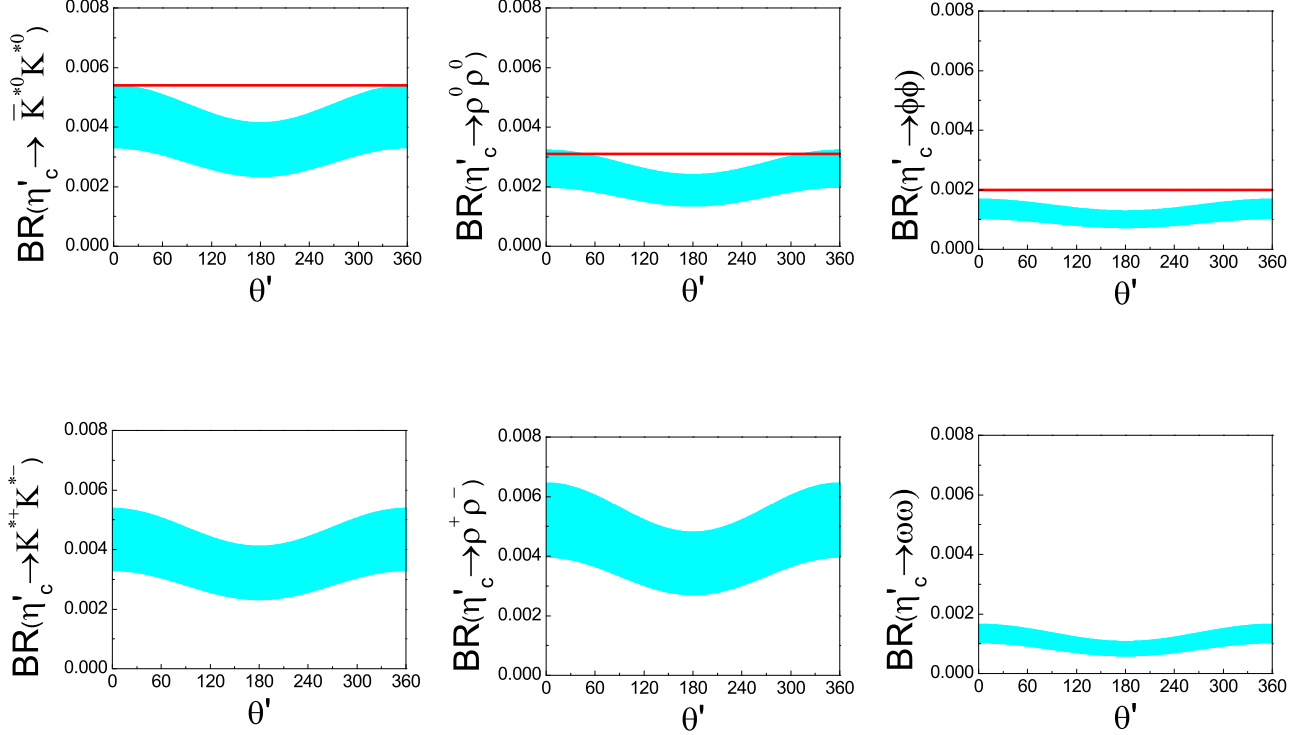


FIG. 3: The  $\theta'$ -dependence of the branching ratios of  $\eta_c' \rightarrow VV$  with  $\alpha_{\eta_c'} = \alpha_{\eta_c} = 0.30$ . The shadowed bands reflect the uncertainties arising from  $|\eta_c'(0)|/|\eta_c(0)| = 0.62 \pm 0.16$ , while the red solid lines indicate the upper limit from the experimental measurement [2].

amplitudes in the  $\eta_c$  and  $\eta_c'$  decays. The predicted branching ratios for  $\eta_c' \rightarrow VV$  turn out to be consistent with the recent data from BES-III [2].

This investigation provides additional information for the IML transitions. Similar to  $J/\psi \rightarrow VP$ , the IML effects are negligible in  $\eta_c \rightarrow VV$  since their masses are far below the open charm thresholds. It was found that the IML transitions played an important role in  $\psi' \rightarrow VP$  since the mass of  $\psi'$  was close to the  $D\bar{D}$  threshold [16]. In contrast, the IML contributions in  $\eta_c' \rightarrow VV$  are not as significant as those in  $\psi' \rightarrow VP$  since the contributing open charm threshold starts with  $D^*\bar{D} + c.c.$  which is much higher than  $D\bar{D}$ . This interesting feature suggests that the same IML mechanism would have rather different manifestations in different processes. We stress that such a correlated study is crucial for disentangling some of those long-standing puzzles in the charmonium energy region.

We should also mention that our conclusions are based on the hypothesis that the flavor components of  $\eta_c$  and  $\eta_c'$  are dominated by  $c\bar{c}$ . Thus, the connection of their spatial wavefunctions with those of  $J/\psi$  and  $\psi'$  will make sense. If  $\eta_c$  or  $\eta_c'$  possesses some other internal structures [7, 8, 35, 36], the relation between their branching ratios will be



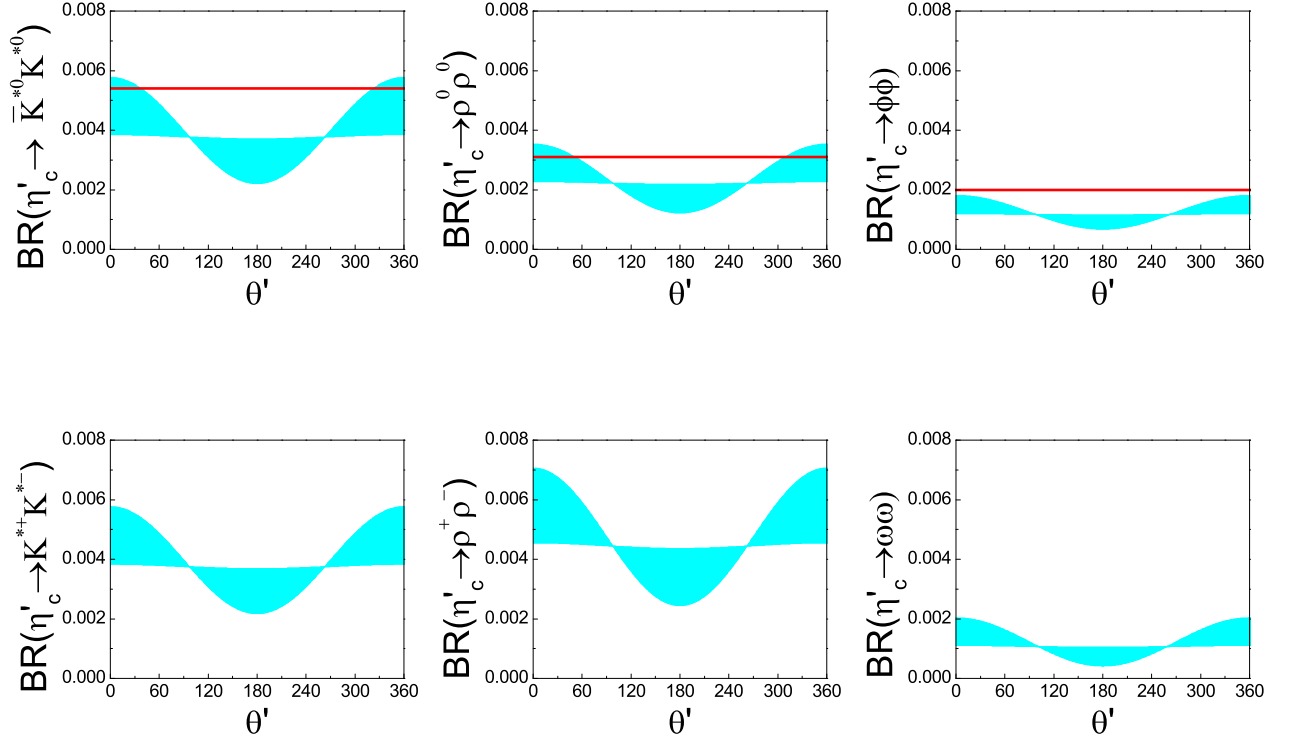


FIG. 4: The  $\theta'$ -dependence of the branching ratios of  $\eta_c' \rightarrow VV$  with  $|\eta_c'(0)|/|\eta_c(0)| = 0.62$ . The shadowed areas reflect the uncertainties arising from  $\alpha_{\eta_c} = 0.30 \pm 0.151$ , while the red solid lines are the same as in Fig. 3.

affected to some extent, which however, is not our focus in this work.

### Acknowledgement

This work is supported, in part, by National Natural Science Foundation of China (Grant No. 11035006), Chinese Academy of Sciences (KJCX2-EW-N01), and Ministry of Science and Technology of China (2009CB825200).

### Appendix

The IML transition amplitudes for the  $\eta_c$  decays into  $\rho\rho$ ,  $K^*\bar{K}^*$ ,  $\omega\omega$ , and  $\phi\phi$  as illustrated by Fig. 2 are presented here for a reference:

$$\begin{aligned} \mathcal{M}(\eta_c \rightarrow \rho^0 \rho^0) = & \mathcal{M}_{D^+ D^{*-} [D^+]} + \mathcal{M}_{D^{*+} D^- [D^{*+}]} + \mathcal{M}_{D^{*+} D^- [D^+]} \\ & + \mathcal{M}_{D^+ D^{*-} [D^{*+}]} + \mathcal{M}_{D^{*+} D^{*-} [D^+]} + \mathcal{M}_{D^{*+} D^{*-} [D^{*+}]} \\ & + \mathcal{M}_{D^0 \bar{D}^{*0} [D^0]} + \mathcal{M}_{D^{*0} \bar{D}^0 [D^{*0}]} + \mathcal{M}_{D^{*0} \bar{D}^0 [D^0]} \\ & + \mathcal{M}_{D^0 \bar{D}^{*0} [D^{*0}]} + \mathcal{M}_{D^{*0} \bar{D}^{*0} [D^0]} + \mathcal{M}_{D^{*0} \bar{D}^{*0} [D^{*0}]} + c.c., \end{aligned} \quad (21)$$

$$\begin{aligned} \mathcal{M}(\eta_c \rightarrow \rho^+ \rho^-) = & \mathcal{M}_{D^+ D^{*-} [D^0]} + \mathcal{M}_{D^{*+} D^- [D^{*0}]} + \mathcal{M}_{D^{*+} D^- [D^0]} \\ & + \mathcal{M}_{D^+ D^{*-} [D^{*0}]} + \mathcal{M}_{D^{*+} D^{*-} [D^0]} + \mathcal{M}_{D^{*+} D^{*-} [D^{*0}]} \\ & + \mathcal{M}_{D^0 \bar{D}^{*0} [D^-]} + \mathcal{M}_{D^{*0} \bar{D}^0 [D^{*-}]} + \mathcal{M}_{D^{*0} \bar{D}^0 [D^-]} \\ & + \mathcal{M}_{D^0 \bar{D}^{*0} [D^{*-}]} + \mathcal{M}_{D^{*0} \bar{D}^{*0} [D^-]} + \mathcal{M}_{D^{*0} \bar{D}^{*0} [D^{*-}]} + c.c., \end{aligned} \quad (22)$$

$$\mathcal{M}(\eta_c \rightarrow \omega\omega) = \mathcal{M}(\eta_c \rightarrow \rho^0 \rho^0), \quad (23)$$

$$\begin{aligned} \mathcal{M}(\eta_c \rightarrow K^{*0} \bar{K}^{*0}) &= \mathcal{M}_{D_s^+ D_s^{*-}[D^+]} + \mathcal{M}_{D_s^{*+} D_s^- [D^{*+}]} + \mathcal{M}_{D_s^{*+} D_s^- [D^+]} \\ &+ \mathcal{M}_{D_s^+ D_s^{*-}[D^{*+}]} + \mathcal{M}_{D_s^{*+} D_s^{*-}[D^+]} + \mathcal{M}_{D_s^{*+} D_s^{*-}[D^{*+}]} \\ &+ \mathcal{M}_{D^- D^{*+}[D_s^-]} + \mathcal{M}_{D^{*-} D^+[D_s^{*-}]} + \mathcal{M}_{D^{*-} D^+[D_s^-]} \\ &+ \mathcal{M}_{D^- D^{*+}[D_s^{*-}]} + \mathcal{M}_{D^{*-} D^{*+}[D_s^-]} + \mathcal{M}_{D^{*-} D^{*+}[D_s^{*-}]} + c.c., \end{aligned} \quad (24)$$

$$\begin{aligned} \mathcal{M}(\eta_c \rightarrow K^{*+} K^{*-}) &= \mathcal{M}_{D_s^+ D_s^{*-}[D^0]} + \mathcal{M}_{D_s^{*+} D_s^- [D^{*0}]} + \mathcal{M}_{D_s^{*+} D_s^- [D^0]} \\ &+ \mathcal{M}_{D_s^+ D_s^{*-}[D^{*0}]} + \mathcal{M}_{D_s^{*+} D_s^{*-}[D^0]} + \mathcal{M}_{D_s^{*+} D_s^{*-}[D^{*0}]} \\ &+ \mathcal{M}_{D^0 \bar{D}^{*0}[D_s^-]} + \mathcal{M}_{D^{*0} \bar{D}^0[D_s^{*-}]} + \mathcal{M}_{D^{*0} \bar{D}^0[D_s^-]} \\ &+ \mathcal{M}_{D^0 \bar{D}^{*0}[D_s^{*-}]} + \mathcal{M}_{D^{*0} \bar{D}^{*0}[D_s^-]} + \mathcal{M}_{D^{*0} \bar{D}^{*0}[D_s^{*-}]} + c.c., \end{aligned} \quad (25)$$

$$\begin{aligned} \mathcal{M}(\eta_c \rightarrow \phi\phi) &= \mathcal{M}_{D_s^+ D_s^{*-}[D_s^+]} + \mathcal{M}_{D_s^{*+} D_s^- [D_s^{*+}]} + \mathcal{M}_{D_s^{*+} D_s^- [D_s^+]} \\ &+ \mathcal{M}_{D_s^+ D_s^{*-}[D_s^{*+}]} + \mathcal{M}_{D_s^{*+} D_s^{*-}[D_s^+]} + \mathcal{M}_{D_s^{*+} D_s^{*-}[D_s^{*+}]} \\ &+ \mathcal{M}_{D_s^- D_s^{*+}[D_s^-]} + \mathcal{M}_{D_s^{*-} D_s^+[D_s^{*-}]} + \mathcal{M}_{D_s^{*-} D_s^+[D_s^-]} \\ &+ \mathcal{M}_{D_s^- D_s^{*+}[D_s^{*-}]} + \mathcal{M}_{D_s^{*-} D_s^{*+}[D_s^-]} + \mathcal{M}_{D_s^{*-} D_s^{*+}[D_s^{*-}]} + c.c. \end{aligned} \quad (26)$$

- 
- [1] D. Cronin-Hennessy *et al.* [CLEO Collaboration], Phys. Rev. D **81**, 052002 (2010) [arXiv:0910.1324 [hep-ex]].
- [2] M. Ablikim *et al.* [BESIII Collaboration], Phys. Rev. D **84**, 091102 (2011) [arXiv:1110.0949 [hep-ex]].
- [3] S. J. Brodsky and G. P. Lepage, Phys. Rev. D **24**, 2848 (1981).
- [4] V. L. Chernyak and A. R. Zhitnitsky, Nucl. Phys. B **201**, 492 (1982) [Erratum-ibid. B **214**, 547 (1983)].
- [5] V. L. Chernyak and A. R. Zhitnitsky, Phys. Rept. **112**, 173 (1984).
- [6] M. Benayoun, V. L. Chernyak and I. R. Zhitnitsky, Nucl. Phys. B **348** (1991) 327.
- [7] M. Anselmino, F. Murgia and F. Caruso, Phys. Rev. D **42**, 3218 (1990).
- [8] M. Anselmino, M. Genovese and D. E. Kharzeev, Phys. Rev. D **50**, 595 (1994) [arXiv:hep-ph/9310344].
- [9] Q. Zhao, Phys. Lett. B **636**, 197 (2006) [arXiv:hep-ph/0602216].
- [10] H. Q. Zhou, R. G. Ping and B. S. Zou, Phys. Rev. D **71**, 114002 (2005).
- [11] E. Braaten, S. Fleming and A. K. Leibovich, Phys. Rev. D **63**, 094006 (2001) [arXiv:hep-ph/0008091].
- [12] P. Santorelli, Phys. Rev. D **77**, 074012 (2008) [arXiv:hep-ph/0703232].
- [13] P. Sun, G. Hao and C. -F. Qiao, Phys. Lett. B **702**, 49 (2011) [arXiv:1005.5535 [hep-ph]].
- [14] Q. Zhao, G. Li and C. H. Chang, Phys. Lett. B **645**, 173 (2007) [arXiv:hep-ph/0610223].
- [15] G. Li, Q. Zhao and C. H. Chang, J. Phys. G **35**, 055002 (2008) [arXiv:hep-ph/0701020]; Q. Zhao *et al.*, Chinese Phys. C **34**, 299 (2010).
- [16] Q. Wang, G. Li and Q. Zhao, arXiv:1201.1681 [hep-ph].
- [17] M. Suzuki, Phys. Rev. D **63**, 054021 (2001).
- [18] A. Seiden, H. F. W. Sadrozinski and H. E. Haber, Phys. Rev. D **38**, 824 (1988).
- [19] Q. Wang, X. -H. Liu and Q. Zhao, arXiv:1010.1343 [hep-ph].
- [20] Q. Zhao, Phys. Rev. D **72**, 074001 (2005) [hep-ph/0508086].
- [21] Q. Zhao, Phys. Lett. B **659**, 221 (2008) [arXiv:0705.0101 [hep-ph]].
- [22] C. Amsler and F.E. Close, Phys. Lett. B **353**, 385 (1995); Phys. Rev. D **53**, 295 (1996).
- [23] F.E. Close and A. Kirk, Phys. Lett. B **483**, 345 (2000).
- [24] F.E. Close and Q. Zhao, Phys. Rev. D **71**, 094022 (2005) [arXiv:hep-ph/0504043].
- [25] Y.-J. Zhang, G. Li and Q. Zhao, Phys. Rev. Lett. **102**, 172001 (2009) [arXiv:0902.1300 [hep-ph]].
- [26] X.-H. Liu and Q. Zhao, Phys. Rev. D **81**, 014017 (2010) [arXiv:0912.1508 [hep-ph]].
- [27] X.-H. Liu and Q. Zhao, J. Phys. G **38**, 035007 (2011) [arXiv:1004.0496 [hep-ph]].
- [28] P. Colangelo, F. De Fazio and T. N. Pham, Phys. Rev. D **69**, 054023 (2004) [arXiv:hep-ph/0310084].
- [29] R. Casalbuoni, A. Deandrea, N. Di Bartolomeo, R. Gatto, F. Feruglio and G. Nardulli, Phys. Rept. **281**, 145 (1997) [arXiv:hep-ph/9605342].
- [30] H. Y. Cheng, C. K. Chua and A. Soni, Phys. Rev. D **71**, 014030 (2005) [arXiv:hep-ph/0409317].
- [31] K. Nakamura *et al.* [Particle Data Group Collaboration], J. Phys. G **G37**, 075021 (2010).
- [32] E. Eichten, K. Gottfried, T. Kinoshita, K. D. Lane and T. -M. Yan, Phys. Rev. D **17**, 3090 (1978) [Erratum-ibid. D **21**, 313 (1980)].
- [33] E. J. Eichten, K. Lane and C. Quigg, Phys. Rev. D **73**, 014014 (2006) [Erratum-ibid. D **73**, 079903 (2006)] [hep-ph/0511179].
- [34] E. J. Eichten, K. Lane and C. Quigg, Phys. Rev. D **69**, 094019 (2004) [hep-ph/0401210].
- [35] Y. -D. Tsai, H. -n. Li and Q. Zhao, Phys. Rev. D **85**, 034002 (2012) [arXiv:1110.6235 [hep-ph]].

- [36] T. Feldmann and P. Kroll, Phys. Rev. D **62**, 074006 (2000) [arXiv:hep-ph/0003096].